Distributions of Local Supply and Exhaust Effectiveness according to Room Airflow Patterns

Hwataik Han*, Sun-Ho Choi** and Woo-Won Lee**

Key words: Ventilation effectiveness, Local mean age, Local mean residual-life-time, Tracer gas technique, Air distribution

Abstract

A pulsed tracer gas technique is applied to measure the distributions of local mean age and local mean residual-life-time of air in a half-scale experimental chamber. The airflow patterns in the chamber are visualized by a Helium bubble generator for three different exhaust locations. A supply slot is located at the top of a right wall, and an exhaust slot is at either bottom-left (Case 1), bottom-right (Case 2), or top-left (Case 3) location. Results show that the distributions of local mean age and local mean residual-life-time are different from each other, but both of them are closely related to the airflow pattern in the space. Included are discussions on explaining the variations of overall room ventilation effectiveness depending upon airflow rates for three different supply-exhaust configurations.

Nomenclature

ACH : air change per hour
C : tracer gas concentration [ppm]
LMA_p : local mean age at point P [sec]
LMR_p : local mean residual-life-time at P [sec]
Q : volumetric airflow rate [m^3/s]
t : time [sec]
V : total volume of the room [m^3]

Greek symbols

ε : ventilation effectiveness
τ_n : nominal time constant ($= V/Q$)
$< >$: room mean value

Subscripts

ex : at exhaust
P : at a point P within a chamber
sup : at supply

* Department of Mechanical and Automotive Engineering, Kookmin University, Seoul 136-702, Korea
** Graduate School, Kookmin University, Seoul 136-702, Korea

1. Introduction

Ventilation is needed to supply fresh outdoor air to an occupied space and to remove air-

borne contaminants generated within the space. In order to quantify ventilation performance, various definitions of ventilation effectiveness have been developed, since Yaglou and Witheridge[1] first introduced the terminology in 1937.

Recently, a concept based on the age of air proposed by Sandberg[2] has been widely accepted. ASHRAE[3] defined local air change index and room air change efficiency based on local mean age and room mean age. Studies have been conducted to develop experimental methods[4] to measure air change efficiency using a tracer gas technique and to develop numerical methods[5] to predict ventilation performance by turbulent airflow calculations using computational fluid dynamics.

However, most of the studies have been focused on the supply of clean ventilation air to a location in a room rather than the removal of contaminants generated indoor. There are some investigations on contaminant removal effectiveness,[6] but they are mostly involved with the overall removal characteristics for specified contaminant sources. Exhaust effectiveness should be defined in parallel with supply effectiveness, both of which should be based on airflow pattern in the space but not on contaminant characteristics.

It is an objective of the present study to investigate the effect of room airflow pattern on exhaust effectiveness. The distributions of local mean residual-life-time and local mean age of air are measured using a pulsed tracer gas technique. The results of exhaust effectiveness based on LMR are compared with those of supply effectiveness based on LMA. The variations of overall room ventilation effectiveness are presented depending upon air change rate as well as upon different supply-exhaust configurations.

2. Theoretical basis

Local supply index or local exhaust index can be defined as the ratio of local mean age of air or local mean residual-life-time of air compared to the nominal time constant of a space. The nominal time constant is the space volume divided by ventilation rate, which is the inverse of air change rate per hour (ACH).

The LMR at a supply means the time duration for a contaminant generated at the supply to reach an exhaust, which has the same meaning with the LMA at exhaust. Both of them are equal to the nominal time constant theoretically.

$$\tau_n = LMA_{ex} = LMR_{sup} \tag{1}$$

The average of LMR over an entire space is room mean exhaust effectiveness, which can be proved to be the same with the room mean supply effectiveness. It is therefore needless to distinguish supply and exhaust effectiveness in overall sense. It can be simply termed as ventilation effectiveness.

$$\langle \varepsilon \rangle = \frac{\tau_n}{2 \cdot \langle LMR \rangle} = \frac{\tau_n}{2 \cdot \langle LMA \rangle} \tag{2}$$

where $\langle\ \rangle$ means the average value over the entire space. The ventilation effectiveness is 50% for complete mixing conditions, and 100% for displacement ventilation conditions.

In order to obtain LMA at a point experimentally, concentration variation needs to be monitored at the point after a tracer is injected at a supply. LMR at a point can be measured by monitoring concentration variation at an exhaust after a tracer is injected at the internal point.

There are three tracer-injection methods to determine LMA or LMR values, i.e. pulse, step-up, and step-down. Following equations of (3) and (4) can be used to compute LMA and LMR values for a pulse method. Room mean age or room mean residual-life-time can be obtained according to equation (5).

$$LMA_P = \frac{\int_0^\infty t \cdot C_P^{sup}(t)\,dt}{\int_0^\infty C_P^{sup}(t)\,dt} \quad (3)$$

$$LMR_P = \frac{\int_0^\infty t \cdot C_{ex}^{P}(t)\,dt}{\int_0^\infty C_{ex}^{P}(t)\,dt} \quad (4)$$

$$\langle LMA \rangle = \langle LMR \rangle = \frac{\int_0^\infty t^2 \cdot C_{ex}^{sup}(t)\,dt}{\int_0^\infty C_{ex}^{sup}(t)\,dt} \quad (5)$$

where the superscripts indicate tracer injection locations, whereas the subscripts indicate the concentration monitoring locations.

3. Experiments

3.1 Experimental apparatus

An experimental chamber used for the present study has dimensions of 1.8 m×1.2 m×0.9 m (L×H×W). There is a supply slot on the top of the right wall, and an exhaust slot at one of three different locations, i.e. bottom-left (Case 1), bottom-right (Case 2), and top-left (Case 3). The supply and the exhaust slots are 0.025 m in width, and supply air discharges horizontally. The ventilation airflow rate is controlled by a variable speed DC motor of a supply fan, and is measured using a 49 mm nozzle in the supply air duct. An exhaust fan is used to maintain the pressure inside the chamber balanced with atmospheric pressure in order to minimize infiltration through the chamber envelope. The exhaust air from the chamber is dumped outside the building not to reentrained into the chamber. The sulfur hexafluoride (SF6) of 30% concentration is used as a tracer gas. Using a syringe, 10 mL of SF_6 is injected into a polystyrene tube, and the gas is mixed with a continuous stream of nitrogen.

The diluted tracer gas is injected at a point in the chamber through a porous sphere of 40 mm in diameter connected at the end of the tube. A tracer gas detector is a multi-gas monitor based on non-disperse infra-red (NDIR) absorption principle. To visualize airflow patterns in the chamber, helium bubbles are discharged into a supply air duct, and a sheet of light is illuminated through the center of the chamber. A schematic diagram of the experimental setup is shown in Fig. 1.

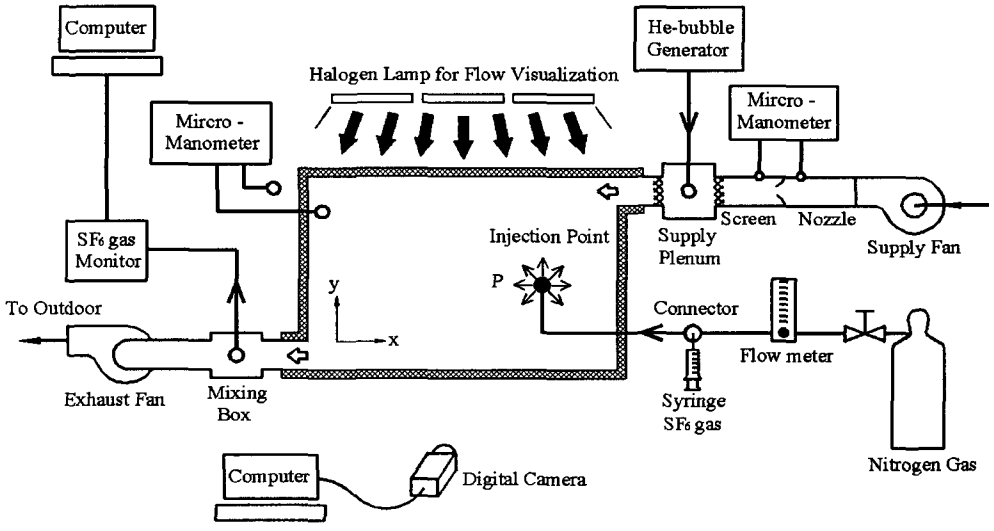

Fig. 1 Schematic of the experimental setup.

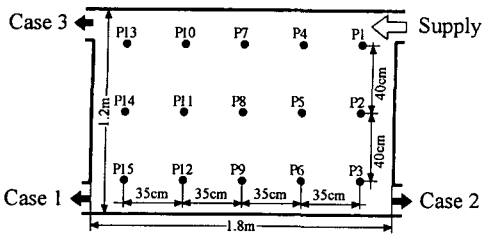

Fig. 2 Locations of tracer injection or concentration monitoring for LMR or LMA measurements.

3.2 Experimental procedure

First of all, the ventilation airflow rate is fixed at 12 ACH. For LMR measurements, tracer gas is injected through a porous sphere at a point in the chamber and then time-dependant tracer gas concentration variation is measured at the exhaust. After the tracer gas is exhausted completely from the chamber, the injection sphere is moved to another point in the chamber. The experimental procedure described above is repeated for all the internal points shown in Fig. 2.

For LMA measurements, all the experimental conditions are identical to the LMR case, but tracer gas is injected at a supply duct and then time-dependant tracer gas concentration variation is measured at the points shown in Fig. 2.

Room mean ventilation effectiveness is calculated from the concentration variations at the exhaust. Experiments are conducted for three different exhaust locations under isothermal room temperature condition. The airflow rate is varied in the range of 4-76 ACH.

4. Results and discussions

4.1 Flow visualization

Flow visualization res are shown in Fig. 3 for three different exhaust locations. The air change rates are 12 ACH's. For Case 1, the air supplied in the horizontal direction moves toward the bottom-left exhaust grille in the diagonal direction. The remaining room air forms two large recirculating flows at top-left and bottom-right corners.

For Case 2, the air supplied along the ceiling changes its direction by the opposite wall and makes a big circulation in the chamber. It can be noticed that the airflow pattern is quite similar to a complete mixing condition. For Case 3, supplied air is facing directly to the exhaust.

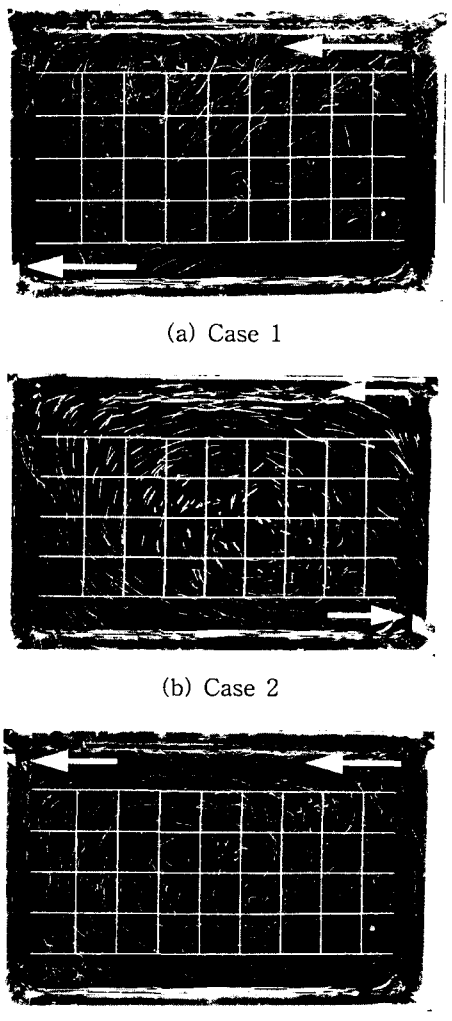

(a) Case 1

(b) Case 2

(c) Case 3

Fig. 3 Flow visualization results for three difference cases.

The room air is mostly stagnant but with a slow recirculation due to the viscous action of the bypass flow.

4.2 LMA and LMR distributions

Fig. 4 shows concentration variations at several points after a pulsed injection applied at supply duct for Case 3. Each curve shows a rapid increase in concentration initially and an exponential decay after a peak. The curve at P8 shows a delay in concentration increase initially, since the point P8 is within the recirculation region at the center of the chamber.

To measure LMR distributions, tracer gas needs to be injected at internal points. Fig. 5 shows concentration variations at exhaust after a pulsed injection applied at several internal points for Case 1. Similar to LMA experiment, each curve shows a rapid concentration increase initially and an exponential decay after a peak.

LMA and LMR values are computed from the concentration curves according to the equation (3) and (4) for all the measuring points. Contours of LMA and LMR are plotted in Fig. 6 for Case 1. It can be seen that both of the distributions are closely related to the airflow pattern visualized in Fig. 3(a). LMA and LMR values are large within recirculating zones. But LMA is small adjacent to supply air inlet and large adjacent to return air grille, whereas LMR is small adjacent to return air grille and large adjacent to supply air inlet. Fig. 7 shows LMA and LMR distributions for Case 2. LMA and LMR distributions are similar to the airflow pattern shown in Fig. 3(b). LMA is relatively small near ceiling, whereas LMR is small near floor.

Both of them have large values within a large recirculation zone at the center.

Fig. 8 shows LMA and LMR distributions for Case 3. LMA and LMR are small near ceiling, and are large adjacent to floor.

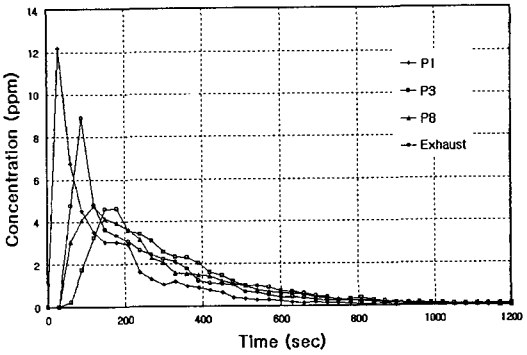

Fig. 4 Transient concentrations at various monitoring points for Case 3.

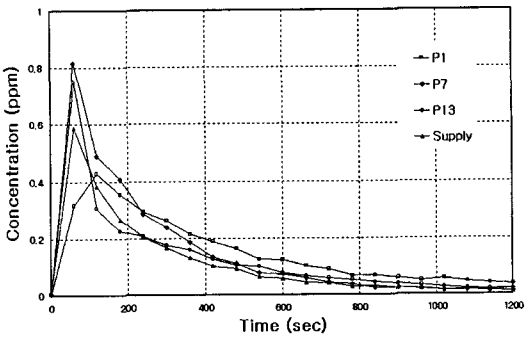

Fig. 5 Transient concentrations at exhaust by various injection points for Case 1.

The airflow pattern, as shown in Fig. 3(c), indicates there is a large stagnant recirculation at lower half of the space. The slow air movement is created passively by the injected supply air along the ceiling. It is considered that the tracer gas diffused to the lower part of the chamber cannot be exhausted effectively.

4.3 Room ventilation effectiveness

Room average ventilation effectiveness is obtained from the concentration variations at exhaust after a tracer injection at supply according to the equation described earlier. Figure 8 shows the room mean ventilation effectiveness for various air change rates. For Case 1, the effectiveness decreases as air change rate increases for low ACH's, but remains nearly con-

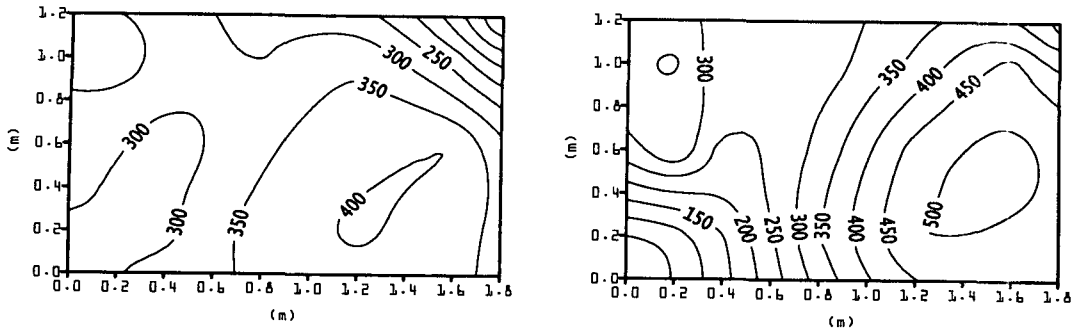

(a) LMA contour (sec) (b) LMR contour (sec)

Fig. 6 LMA and LMR distribution for Case 1.

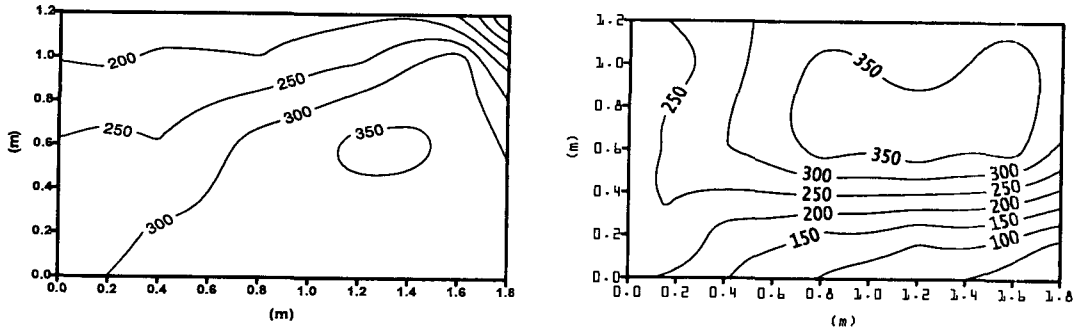

(a) LMA contour (sec) (b) LMR contour (sec)

Fig. 7 LMA and LMR distribution for Case 2.

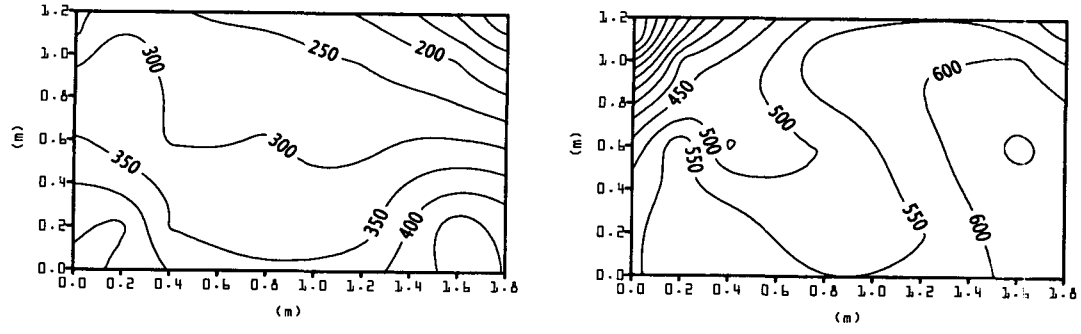

(a) LMA contour (sec) (b) LMR contour (sec)

Fig. 8 LMA and LMR distribution for Case 3.

stant for ACH greater than 20 approximately. The ventilation effectiveness is between 0.4~0.5, which is similar to a complete mixing condition. For Case 2, as the air change rate increases, the effectiveness increases initially and decreases slowly afterwards. The effectiveness remains nearly constant for over 20 ACH as Case 1. However, the ventilation effectiveness in Case 3 is significantly lower compared to Case 1 and Case 2, especially in low range of ACH's. It is due to the fact that the supply jet is facing directly to the exhaust, and that remaining room air is mostly stagnant but with a slow recirculation.

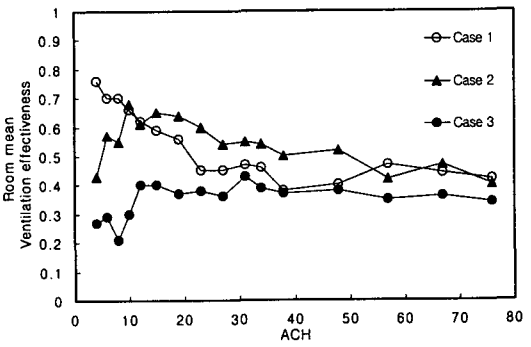

Fig. 9 Effect of ACH on room mean ventilation effectiveness.

5. Conclusions

In order to study supply and exhaust effectiveness according to airflow pattern, tracer gas experiments have been performed in a half-scale ventilation chamber.

(1) The distributions of LMA and LMR show different characteristics from each other, but both of them are closely related to the airflow pattern in the space.

(2) LMA is small adjacent to supply inlet, and large adjacent to return-air exhaust, whereas LMR is small adjacent to return-air exhaust, and large adjacent to supply air inlet.

(3) Compared to Case 1 and Case 2, Case 3 where the exhaust is located at the direct opposite side of the supply, shows poor overall room ventilation effectiveness over the range of ACH investigated in the present study.

(4) The overall ventilation effectiveness depends not only on supply-exhaust configurations, but also on air change rate.

The concept of local mean residual-life-time of air can be used in designing the locations of contaminant sources in a building such as a smoking zone, whereas that of local mean age can be used in designing proper distribution of fresh supply air into an occupied zone.

Acknowledgements

This paper has been funded by Korea Science and Engineering Foundation under the grant of KOSEF 1999-2-310-003-3.

References

1. Yaglou, C. P. and Witheridge, W. N., 1937, Ventilation Requirements, ASHVE Trans., Vol. 42, pp. 423-436.
2. Sandberg, M. and Sjoberg, M., 1983, The Use of Moments for Assessing Air Quality in Ventilated Rooms, Building and Environment, Vol. 18, No. 4, pp. 181-197.
3. ASHRAE, 1997, ASHRAE Handbook-Fundamentals, American Society of Heating, Refrigerating, and Air-Conditioning Engineers.
4. ASHRAE, 1997, Measuring Air-Change Effectiveness, ANSI/ASHRAE 129-1997, American Society of Heating, Refrigerating, and Air-Conditioning Engineers, Atlanta.
5. Han, H., 1992, Numerical Analysis of Ventilation Effectiveness using Turbulent Airflow Modeling, Proc. of Int. Symp. on Room Air Convection and Ventilation Effectiveness, pp. 187-191.
6. Faulkner, D., Fisk, W. J., Sullivan, D. P. and Wyon, D. P., 1999, Ventilation efficiencies of Desk-Mounted Task/Ambient Conditioning Systems, Indoor Air, Vol. 9, No. 4, pp. 273-281.
7. Han, H., Kuehn, T. H. and Kim, Y. I., 1999, Local Mean Age Measurements for Heating, Cooling, and Isothermal Supply Air Conditions, ASHRAE Trans., Vol. 105, Pt. 2, pp. 275-282.